Comparison of Measured and Theoretical Scattering and Polarization Properties of Narrow Size Range Irregular Sediment Particles

Wayne Homer Slade, Yogesh C. Agrawal, and Ole A. Mikkelsen
Sequoia Scientific, Inc.
Bellevue, WA,USA
wslade@sequoiasci.com

***Abstract*—The predominant use of theoretical models for angular light scattering due to particles is largely due to limited number of actual measurements. Measuring the angular scattering is difficult due to the wide dynamic range of intensity as a function of angle, as well as variability across particle types and environments. The present work continues ongoing research by the authors related to the scattering properties of irregular particles. Using the recently developed LISST-VSF instrument, we measured the VSF at angles from approximately 0.1 to 150 degrees, as well as the degree of linear polarization from 15 to 150 degrees, of narrow size distributions of irregular silt and sand-sized particles (Arizona Test Dust) in the laboratory. The general trend in these observations is as expected: larger particles become more strongly peaked in the near-forward angles. , The measured phase functions also had greatly enhanced scattering in the mid angles, approximately 40 to 100 degrees, compared with the Petzold phase functions. Measured degree of linear polarization was significantly different from theoretical predictions, likely due to particle shape and composition.**

Keywords—ocean optics; light scattering; phase function; particle scattering; polarized scattering

I. INTRODUCTION

The scattering phase function ($\tilde{\beta}(\psi)$, units of sr^{-1}, where ψ is the scattering angle with $\psi = 0$ defined as forward) of particles describes the angular distribution of non-polarized light scattered from an incident beam [1−2]. The phase function is essential in determining the light distribution in-water (for example in visibility or beam propagation studies) and leaving the surface (such as towards a remote-sensing instrument). The ocean optics research community has relied on approximations to the phase function based on theoretical models and a limited dataset of measurements [3]. The most commonly used model, Mie theory, is a computationally-convenient tool for understanding first-order particle optical properties, but marine particles are usually highly non-spherical, and Mie theory is known to be particularly unsuitable for non-spherical particles. For instance, the oscillations of the phase function predicted by Mie theory vanish for irregular particles in the small, mid- and backscattering angles [4−6]; and even the roughness of otherwise spherical particles has been shown to have profound effects on scattering especially in the backscattering angles [7]. Other models such as layered spheres [8], T-Matrix [5], and the Improved Geometric Optics Model (IGOM) [9] have also been used, but are typically limited to particular geometries and small particle sizes due to numerical and computation time issues.

Measuring the phase function is challenging due to the wide dynamic range of scattered intensity as a function of angle. Legacy instruments employed a swinging-arm design to measure the scattering at angles about a fixed sample volume. These systems tended to be very large, not easily deployable at sea, had limitations on measurement angles due to instrument geometry, and had very long measurement acquisition times. Due to these engineering challenges in developing instrumentation, most ocean optics research has relied on limited measurements, most commonly those of Petzold [10]. Other key measurements of the angular scattering have been made in the laboratory, usually on cultured phytoplankton [6], [11−13], but also in once instance of silts [11], and also in situ [14−15]. More recently, in situ-capable angular scattering sensors have been developed and deployed by other researchers [9,16−17].

The scattering of light is almost always a polarizing event, i.e., the state of light scattered by particles is altered from the state of the incident light. The polarizing properties of scattering can be measured by using various combinations of polarization filters in the incident and scattered light paths [18]. The degree of linear polarization, P_{12} , describes the amount of incident light that is partially polarized upon scattering; positive if partially polarized perpendicular relative to the scattering plane, negative if parallel to the scattering plane.

II. LISST-VSF INSTRUMENT

The LISST-VSF (Fig. 1) is a submersible instrument for measuring the angular scattering in situ, including polarization discrimination capability. The instrument covers the angular range from ~0.1−150° in water. The range ~0.1−15° is covered with a LISST-100X standard ring detector (50-mm focal length) [4,19−20]. The larger angles, ~15−150° in 1° degree increments, are covered by a 'roving eyeball'. The eyeball is set to one side of the sample volume. As it rotates, the eyeball views scattering from points along the laser beam within the

978-0-933957-40-4 ©2013 MTS

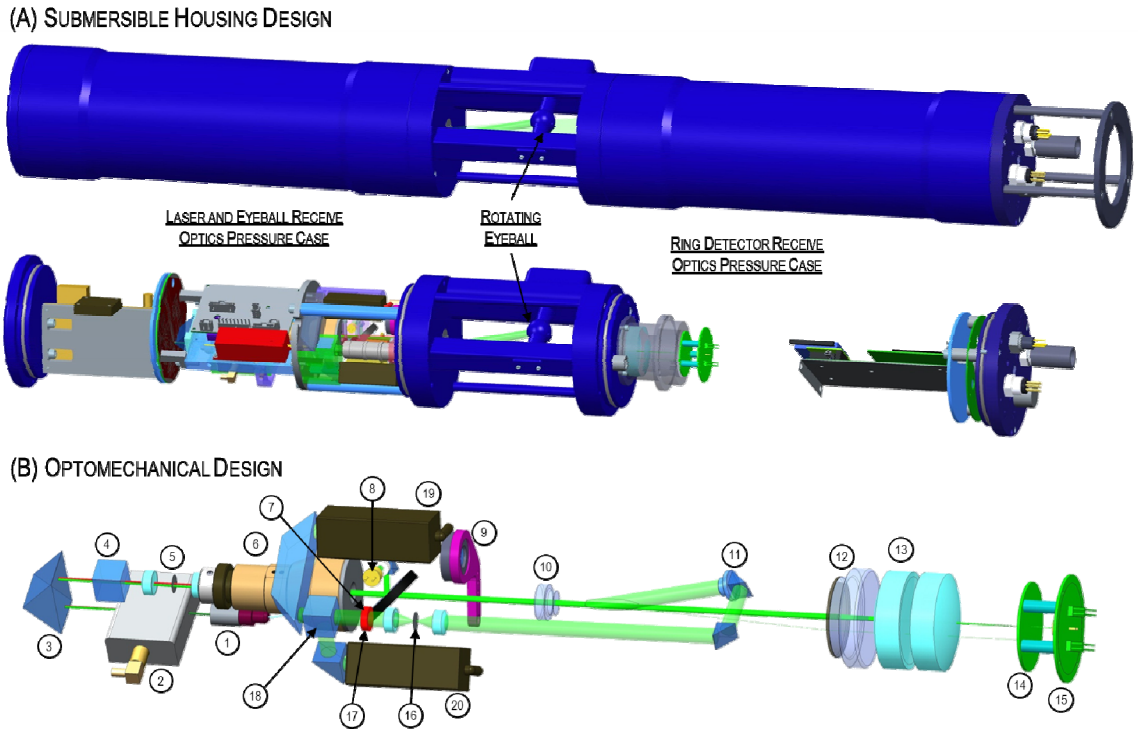

Fig. 1. The LISST-VSF instrument. (A) The left pressure case houses the laser optics, AOM, eyeball PMTs and receive optics, and eyeball motor. The right pressure case houses the ring detector receive optics and microcontroller for instrument control and data storage. Bulkhead connections for power and serial communications are located on the ring detector receive optics pressure case, as well as an external on-off switch. (B) The LISST-VSF optical design consists of a 1 mm diameter green (532 nm) laser beam originating from a TEC laser module (1), passing through an AOM (2), then folded by a prism (3) onto the primary instrument optical axis. The default laser polarization is determined by a polarizing beamsplitter (4). Only the diffracted (modulated) AOM beam is passed by an iris (5) and then expanded to 3 mm (6). The expanded beam is sampled (7) to measure reference laser power by a photodiode (8). A half-wave plate (9) can be mechanically inserted into the laser beam to change the incident polarization between perpendicular and parallel. The beam then passes through the pressure window (10) into water within the sample volume. Behind the receive side pressure window covered in ND glass (12) is the receive lens (13). This lens focuses the scattered light on to the ring detector (14), and the focused beam passes through a central hole to a photodiode (15) which measures beam transmission. The eyeball (11) views scattered light from the sample volume, first passing through a spatial filter (16) to limit the viewing angle of the eyeball, and then an interference filter (17) allowing only light at the laser wavelength. Received scattered light is then split into parallel and perpendicular polarization components by the beamsplitter (18) and measured by the two PMT modules (19) and (20).

sample volume, from about 10° to about 150°. The received scattered light is split into its two polarization components and sensed by separate photomultiplier tubes (PMT), and the incident beam polarization is alternated for each rotation of the eyeball by insertion of a half-wave plate into incident laser beam. An acousto-optical modulator (AOM) allows the intensity of the incident laser beam to be varied during the eyeball rotation in order to avoid saturation of the PMT due to the large dynamic range in scattering phase function. Thus, a single measurement consists of recording the two PMT outputs (parallel and perpendicular polarized scattering) over two rotations of the eyeball with incident laser polarization is perpendicular and then parallel. This permits extraction of the scattering phase function and degree of linear polarization. The rotating eyeball design makes the LISST-VSF instrument compact, autonomous, and easily deployed in situ.

III. PARTICLE MEASUREMENTS

Results presented here were obtained in the laboratory by wrapping the sample volume with a flexible sheet, forming a cylinder with the top left open so that sample water and test particles could be introduced. This setup did not include an automated means to mix particles within the sample volume, thus tests were limited to polystyrene beads and small-size test dusts. The particles analyzed are indicated in Table 1. The sample volume was filled with degassed 0.2-µm filtered water, and samples were ultrasonicated for 180 seconds before addition to the sample volume. In the case of the Arizona Test Dust and 0.33-µm beads, slurries were created from the dry powder or high concentration suspension, ultrasonicated, and then added in small additions to the LISST-VSF sample volume. Measurements were made on suspensions with beam attenuation of approx. 1−2 m^{-1} for ample signal to noise while maintaining single scattering.

LISST-VSF measurements are compared with the results of Mie theory for particles with similar size distribution and refractive index. For the polystyrene spherical beads, a range of refractive indices and uncertainty in the particle size distribution is used to generate a database of predicted scattering curves. Refractive index estimated from the dispersion relationship published by the microsphere manufacturer (Duke Scientific) is 1.60, however, a wider range of values can found in the literature. In this analysis a range of approximately 1.585 to 1.60 [21−22] is assumed. The

TABLE I. PARTICLES ANALYZED USING THE LISST-VSF. REFRACTIVE INDEX AND PARTICLE SIZE DISTRIBUTION ESTIMATES USED IN MIE THEORY FOR COMPARISON ARE ALSO PROVIDED.

Nominal Size	Description	Particles Size Distribution
0.33 µm	Polystyrene Spheres	Gaussian: mean = 0.33 µm, 3% CV
1.03 µm	Polystyrene Spheres	Gaussian: mean = 1.03±0.015 µm, std. dev. 0.010 µm, 1% CV
2–4.5 µm	Arizona Dust	Log-normal, nom. size range is approx. 5th and 95th percentiles. Actual size distribution determined by PTI using Coulter Multisizer and digitized.
2–6 µm	Arizona Dust	
4–8 µm	Arizona Dust	
6–11 µm	Arizona Dust	
10–20 µm	Arizona Dust	
20–30 µm	Arizona Dust	

imaginary part of the index of refraction was assumed negligible based on previous simulations [20]. Particle size distributions for the beads is assumed Gaussian, with standard deviation and variability in mean diameter as specified by the manufacturer.

The irregular particles are Arizona Test Dust Fractions (Powder Technology, Inc., "PTI"). The particles are irregular mineral particles sorted from ISO-12301-1 test powders. They are dominated by SiO_2 (68–76% mass) and Al_2O_3 (10–15% mass), with refractive indices of ~1.55 and ~1.76–1.78, respectively. Based on crude approximation, a refractive index for the mixture is found to be 1.60–1.63. The imaginary part of refraction for the Arizona Dust is assumed negligible as described by Agrawal and Mikkelsen [4]. Particle size distributions for the PTI test dust fractions were measured by Coulter counter and were provided by the manufacturer. The provided volume percent distributions from the Coulter counter were digitized in MATLAB and converted to number distribution by rebinning the log-spaced distributions to uniform linear spacing and by assuming spherical particle geometry.

For all Mie runs, the index of refraction of the pure water is assumed to be 1.335. A fast, vectorized Mie code, fastmie.m [20] based on BHMIE [18], was used.

IV. RESULTS

A. *Polystyrene Microspheres*

Results for the Duke polystyrene microspheres are shown in Fig. 2. Mie theory phase functions and degree of polarization are shown for each bead. In the phase function plots, LISST-VSF measurements are shown offset vertically for clarity. Overall agreement in the shape of phase function between the observations and theoretical results is reasonable compared to the uncertainty in the structure calculated using Mie theory for uncertainties in particle size distributions and indices of refraction. Some stability issues were observed with the polystyrene beads, especially the 0.33 µm, with repeated measurements sometimes exhibiting different structure analogous to changes in size distribution. The nature of this variability remains to be determined, but may be similar to problems mentioned by Lee and Lewis [17], and might be due

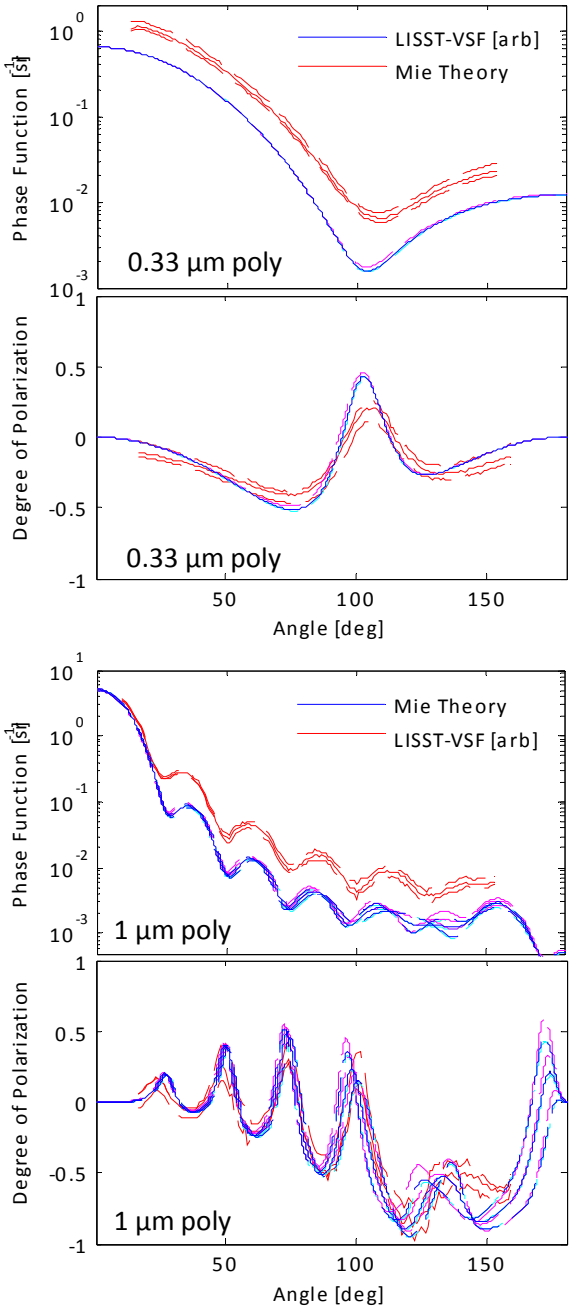

Fig. 2. Comparison of LISST-VSF measurements and Mie theory for 0.33-µm and 1.034-µm polystyrene microspheres. Red curves (offset for clarity) are LISST-VSF measurements and blue, magenta, and cyan curves are Mie theory. Uncertainty in LISST-VSF measurements is shown with dashed red lines. Uncertainty in Mie results due to uncertainty in size (solid vs. dashed) and index of refraction (magenta and cyan) is also shown.

to low stability (i.e., aggregation) of the beads in spite of dispersant and ultrasonication. Variability in the LISST-VSF measurements include fluctuations in the measurement (e.g., electronic noise, rare large particles or bubbles, and particle and density inhomogeneities in the sample), as well as repeated processing of the raw data by assuming multiple values of the

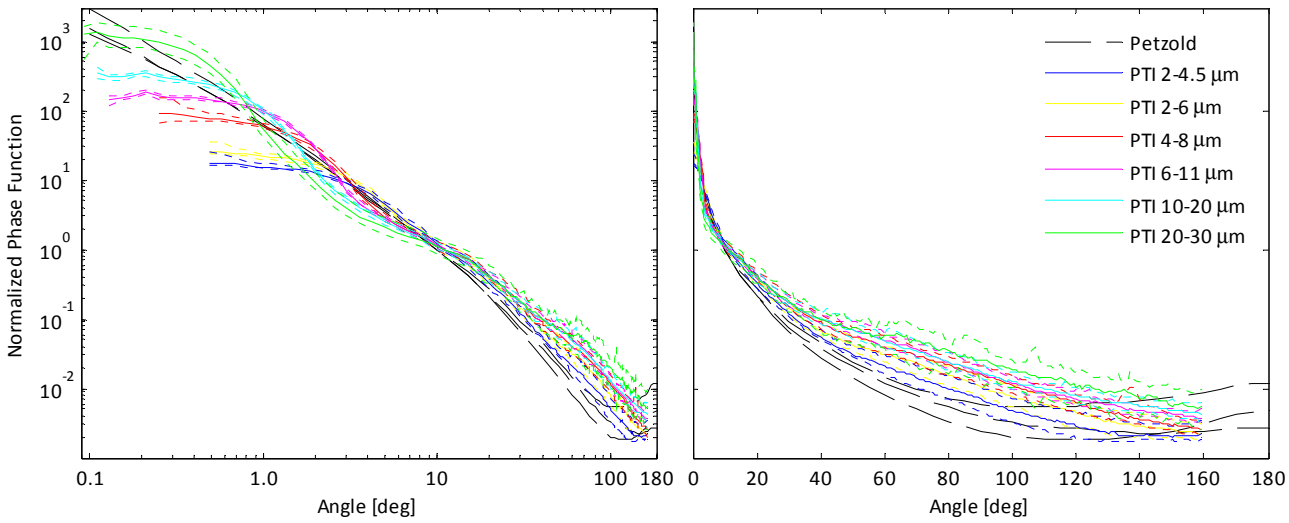

Fig. 3. Measured phase functions (normalized to magnitude at 10°) for the measured PTI Arizona Dust size fractions from Table I. Petzold mean phase functions for clear, coastal, and turbid waters are shown in black dashed.

PMT relative gain (to indicate sensitivity to uncertainty in this parameter).

B. Irregular-shaped Sediment Particles

Measured phase functions for the PTI powders are shown in Fig. 3, along with Petzold mean phase functions [10] as a reference. The general trend in these observations is as expected: Larger particles become more strongly peaked in the near-forward angles. Larger particles also appear to exhibit enhanced scattering compared to smaller particles, and in all cases, the measured phase functions had greatly enhanced scattering in the mid angles (~40−100°) compared with the Petzold phase functions. The 2–4.5 and 2–6 µm appear smooth as functions of angle, while the larger sizes present increasingly obvious inflection points in near-forward angles less than ~20°. A closer look at two of the PTI samples is shown in Fig. 4. The shapes of the measured phase functions are similar to theoretical predictions to first order, however, the structure presented in the near-forward angles mentioned above appears muted compared to Mie theory, not surprising from previous measurements of near-forward scattering by irregular mineral particles [4]. The most striking difference between the measured and theoretical phase functions is the enhancement at mid angles. Degree of linear polarization P_{12} measured and predicted for the 2–4.5 µm, 4–8 µm, and 10–20 µm Arizona Dust size fractions is shown in Fig. 5. Mie theory predictions for P_{12} indicate a change in slope from ~60° to ~120°, becoming steeper with increasing particle size. All three sizes are predicted to have minima near 130° before tending towards zero, though erratically, as angles approach 180°. In contrast, measurements are very dissimilar to the theoretical predictions. The slope of measured P_{12} as it approaches its minima at intermediate angles does not exhibit the same trend with size as predicted, and the shape of the curve in the backwards direction is markedly smoother than theoretical predictions. This smooth structure is similar to a number of previous studies [6,14−15], however, in these previous results, the minima in P_{12} was near 90°. Our observations show a size dependence on the angle position of this minima with no clear relation to size.

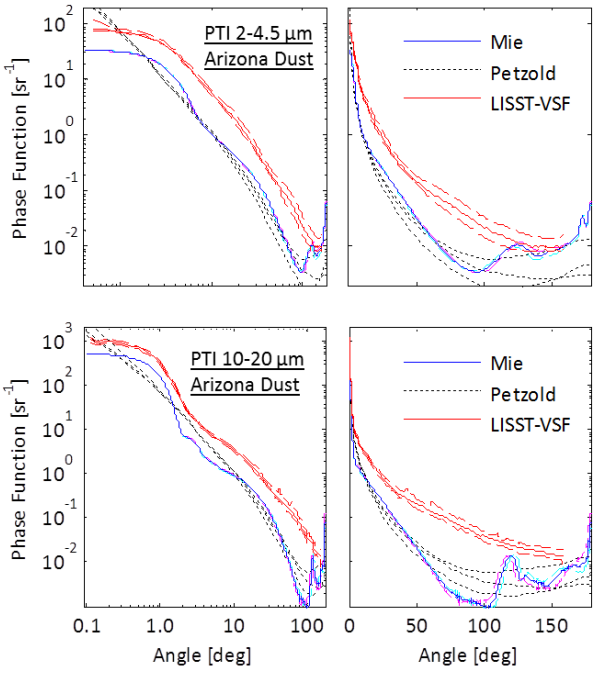

Fig. 4. Measured phase functions for the PTI Arizona Dust 2–4.5 µm (top panels) and 10–20 µm (bottom) size fractions. Red curves are LISST-VSF measurements, offset for clarity. Uncertainty in LISST-VSF measurements is shown with dashed red lines. Uncertainty in Mie results due to uncertainty in index of refraction is shown in magenta and cyan. Petzold mean phase functions for clear, coastal, and turbid waters are shown in black dotted curves.

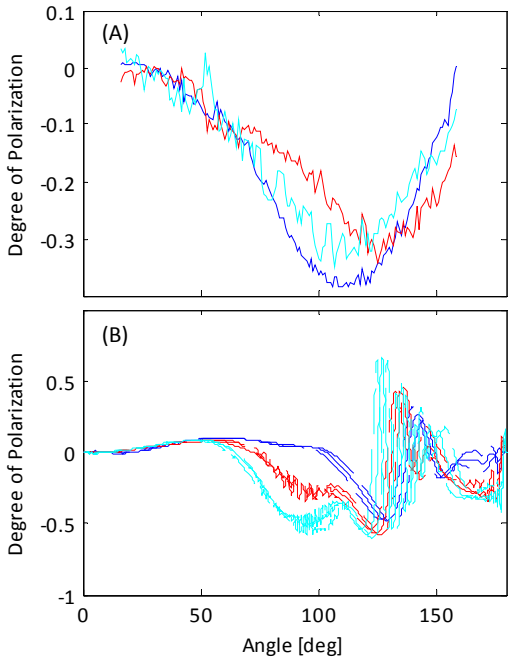

Fig. 5. (A) Measured degree of polarization, P_{12} for the PTI Arizona Dust 2–4.5 µm (blue), 4–8 µm (red), and 10–20 µm (cyan) size fractions. (B) Corresponding Mie theory predictions. Uncertainty in index of refraction is shown in the Mie plot with dashed lines.

V. Summary and Key Findings

A submersible, easily field-deployable, volume scattering function (VSF) sensor, the LISST-VSF, has been developed. The instrument uses a rotating "eyeball" to scan along a laser beam, sensing scattered light in two different polarizations, and with two different incident beam polarizations. These measurements allow calculation of the upper quadrant of the Mueller scattering matrix. Lab measurements of polystyrene microspheres are in good agreement with Mie theory for homogenous spherical particles.

Irregular mineral particles of several relatively narrow size distributions were measured with the LISST-VSF instrument. These measurements agreed to first order with Mie theory predictions for near-forward angles, with deviation increasing with increasing angle. The measured suspensions exhibited scattering at mid angles that was greatly enhanced compared to predictions. Smoothing of VSF structure in the irregular particle suspensions compared with theory was also observed.

Measured degree of polarization P_{12} was significantly different from theoretical predictions. Particle shape and possibly composition appear to have drastic effects on the polarization due to scattering. Observed P_{12} had smooth shapes and minima between 100−125°, in contrast with previous measurements on phytoplankton, silts, and ocean waters that typically had minima near 90°.

Acknowledgment

Construction of the LISST-VSF was supported by the NASA SBIR program.

References

[1] Mobley, Light and Water: Radiative Transfer in Natural Waters. San Diego, CA: Academic Press, 1994.

[2] M. Jonasz and G. Fournier, Light scattering by particles in water: theoretical and experimental foundations. Academic Press, 2007.

[3] C. D. Mobley, L. K. Sundman, and E. Boss, "Phase function effects on oceanic light fields," Applied Optics, vol. 41, no. 6, pp. 1035–1050, Feb. 2002.

[4] Y. C. Agrawal and O. A. Mikkelsen, "Empirical forward scattering phase functions from 0.08 to 16 deg. for randomly shaped terrigenous 1-21 µm sediment grains," Optics Express, vol. 17, no. 11, pp. 8805–8814, May 2009.

[5] W. R. Clavano, E. Boss, and L. Karp-Boss, "Inherent optical properties of non-spherical marine-like particles -- from theory to observation," Oceanography and Marine Biology: An Annual Review, vol. 45, pp. 1–38, 2007.

[6] Ø. Svensen, J. J. Stamnes, M. Kildemo, L. M. S. Aas, S. R. Erga, and Ø. Frette, "Mueller matrix measurements of algae with different shape and size distributions," Applied Optics, vol. 50, no. 26, pp. 5149–57, Sep. 2011.

[7] R. Killinger and R. Zerull, "Effects of shape and orientation to be considered for optical particle sizing," in in Optical Particle Sizing: Theory and Practice, G. Gouesbet and G. Gréhan, Eds. Plenum Press, 1988, pp. 419–429.

[8] X. Zhang, M. Lewis, M. Lee, B. Johnson, and G. Korotaev, "The volume scattering function of natural bubble populations," Limnology and Oceanography, vol. 47, no. 5, pp. 1273–1282, 2002.

[9] M. Twardowski, X. Zhang, and S. Vagle, "The optical volume scattering function in a surf zone inverted to derive sediment and bubble particle subpopulations," Journal of Geophysical Research, 2012.

[10] T. J. Petzold, "Volume scattering functions for selected ocean waters," Scripps Institute of Oceanography SIO Ref. 72-78, 1972.

[11] H. Volten, J. F. De Haan, J. W. Hovenier, R. Schreurs, W. Vassen, F. Charlton, and R. Wouts, "Laboratory measurements of angular distributions of light scattered by phytoplankton and silt," Limnology and Oceanography, vol. 43, no. 6, pp. 1180–1197, 1998.

[12] R. D. Vaillancourt, C. W. Brown, R. L. Guillard, and W. M. Balch, "Light backscattering properties of marine phytoplankton: relationships to cell size, chemical composition and taxonomy," Journal of Plankton Research, vol. 26, no. 2, pp. 191–212, Feb. 2004.

[13] E. S. Fry and K. J. Voss, "Measurement of the Mueller matrix for phytoplankton," Limnology and Oceanography, vol. 30, no. 6, pp. 1322–1326, 1985.

[14] K. J. Voss and E. S. Fry, "Measurement of the Mueller matrix for ocean water," Applied Optics, vol. 23, no. 23, pp. 4427–39, Dec. 1984.

[15] G. F. Beardsley, Jr., "Mueller scattering matrix of sea water," Journal of the Optical Society of America, vol. 58, no. 1, p. 52, Jan. 1968.

[16] J. M. Sullivan, M. S. Twardowski, P. L. Donaghay, and S. a Freeman, "Use of optical scattering to discriminate particle types in coastal waters," Applied Optics, vol. 44, no. 9, pp. 1667–80, Mar. 2005.

[17] M. Lee and M. Lewis, "A new method for the measurement of the optical volume scattering function in the upper ocean," Journal of Atmospheric and Oceanic Technology, vol. 20, pp. 563–572, 2003.

[18] C. F. Bohren and D. R. Huffman, Absorption and Scattering of Light by Small Particles. New York: John Wiley & Sons, 1983.

[19] Y. C. Agrawal, "The optical volume scattering function: Temporal and vertical variability in the water column off the New Jersey coast," Limnology and oceanography, vol. 50, no. 6, pp. 1787–1794, 2005.

[20] W. H. Slade and E. S. Boss, “Calibrated near-forward volume scattering function obtained from the LISST particle sizer,” Optics Express, vol. 14, no. 8, pp. 3602–3615, 2006.

[21] X. Ma, J. Q. Lu, R. S. Brock, K. M. Jacobs, P. Yang, and X.-H. Hu, “Determination of complex refractive index of polystyrene microspheres from 370 to 1610 nm,” Physics in Medicine and Biology, vol. 48, pp. 4165–4272, Dec. 2003.

[22] I. Nikolov and C. Ivanov, “Optical plastic refractive measurements in the visible and the near-infrared regions,” Applied Optics, 2000.